A relaxation scheme to compute three-phase flow models

Jean-Marc Hérard

▶ **To cite this version:**

Jean-Marc Hérard. A relaxation scheme to compute three-phase flow models. 18th AIAA Computational Fluid Dynamics Conference, American Institute Aeronautics and Astronautics, Jun 2007, New Orleans, United States. pp.1647-1657, 10.2514/6.2007-4455 . hal-01582664

HAL Id: hal-01582664
https://hal.science/hal-01582664v1

Submitted on 5 Apr 2018

HAL is a multi-disciplinary open access archive for the deposit and dissemination of scientific research documents, whether they are published or not. The documents may come from teaching and research institutions in France or abroad, or from public or private research centers.

L'archive ouverte pluridisciplinaire **HAL**, est destinée au dépôt et à la diffusion de documents scientifiques de niveau recherche, publiés ou non, émanant des établissements d'enseignement et de recherche français ou étrangers, des laboratoires publics ou privés.

A Relaxation Scheme To Compute Three-Phase Flow Models

Jean-Marc Hérard *

EDF-R&D, 78401 Chatou cedex, France

We provide in this paper a simple algorithm that enables to tackle unsteady three-phase flows. The basic ideas rely on the use of relaxation techniques, and are applied to an hyperbolic three-phase flow model. The scheme may be used to compute either the single-pressure model or the multi-pressure model.

I. Introduction

Some applications in the nuclear industry and in petroleum engineering require the prediction of three-phase flows or at least three-field models. In the nuclear power industry, this may occur for instance inside the core of a Pressurised Water Reactor (PWR) when some reflooding occurs, or when predicting the boiling crisis. In pipelines, the mixture of gas, water and oil also provides a natural framework for these three-phase flow models. Some models are available in the standard literature for porous media (see for instance[5,9]) , which are more or less devoted to the computation of these patterns in reservoirs. These are based on simplified forms of momentum equations, and also assume some rather restrictive conditions on thermodynamics. They are thus not suitable for our purposes: during the rewetting phase after a Loss Of Coolant Accident (LOCA) in a PWR, the main mechanisms are driven by the energy equations, and beyond this by the full governing equations for the momentum. The mass balance equations are of course also needed to control the whole process. Hence, a reasonable approach should take into account nine equations at least, and this will correspond to the classical three-phase flow models, which are refered to as three-field models in[26] .

Owing to the possible loss of hyperbolicity of the latter models, we have derived a slightly different formalism which no longer assumes an instantaneous pressure equilibrium between the three phases, and meanwhile enables to recover a complete set of hyperbolic states, which renders the initial value problem well-posed. Nonetheless, for industrial purposes, it seems tempting to find a uniform formalism that will allow the computation of both approaches in the same numerical procedure. This is precisely the core of the paper, which takes its basics on a father model (corresponding to the second approach) which enables to retrieve formally the first (still more widespread) approach.

The paper is organised as follows:

- We start with a brief presentation of the classical three-phase flow models,
- We then summarize the main patterns of the new framework of hyperbolic three-phase flow models that sustain the relaxation method,
- We eventually provide the guidelines of the numerical procedure, with applications.

II. The classical three-phase flow model

Most of three-phase flow models available in the literature rely on the classical pressure equilibrium approach (see[26] for instance and references therein). If the mean pressure in the flow is noted P, the governing set of equations will read (for $k = 1, 2, 3$):

*Senior Engineer, Département MFEE, 6 quai Watier

$$\alpha_1 + \alpha_2 + \alpha_3 = 1 \tag{1}$$

$$\frac{\partial \alpha_k \rho_k}{\partial t} + \frac{\partial \alpha_k \rho_k U_k}{\partial x} = 0 \tag{2}$$

$$\frac{\partial \alpha_k \rho_k U_k}{\partial t} + \frac{\partial \alpha_k \rho_k U_k^2}{\partial x} + \alpha_k \frac{\partial P}{\partial x} = S_{U_k} \tag{3}$$

$$\frac{\partial \alpha_k E_k}{\partial t} + \frac{\partial \alpha_k U_k (E_k + P)}{\partial x} + P \frac{\partial \alpha_k}{\partial t} = V_i S_{U_k} \tag{4}$$

with the constraint :

$$S_{U_1}(W) + S_{U_2}(W) + S_{U_3}(W) = 0 \tag{5}$$

Standard notations have been used here, for $k = 1, 2, 3$: α_k, ρ_k, $m_k = \alpha_k \rho_k$, U_k and $\alpha_k E_k$ respectively denote the volume fraction, the density, the mass fraction, the mean velocity and the total energy within each phase labelled k. Moreover, the relation $\alpha_k E_k = m_k e_k(P, \rho_k) + m_k U_k^2/2$ holds within each phase, and must be accompanied by an explicit closure law (Equation Of State) for the mean internal energy $e_k(P, \rho_k)$. Standard relations enable to express the drag coefficients, depending on the particular context (Stokes law, Ergun law, ...). Of course, one may account for mass transfer terms in some situations encountered in nuclear applications.

The main properties of the above mentionned model are not clearly identified. The structure of the mass balance equations ensures that the mass fractions will remain positive, assuming that no mass transfer occurs and restricting to smooth solutions, and provided that the mean velocity field and its divergence remain bounded over a compact set $\Omega \times [0, T]$. For phase isentropic situations, this allows to prove that both the void fractions and the mean pressure remain positive, if initial conditions and inlet boundary values are physically relevant. This result may be extended to the framework including mass transfer terms, at least for a particular class of closures.

Nonetheless, no theoretical result is available when shocks are present in the solution, since the occurence of non-conservative terms inhibits the derivation of meaningful jump relations. More over, nothing can be said about the well-posedness of the initial value problem, and it is well-known that the characteristic eigenvalues of the associated convective subset admit a very wide domain of physical states which render the imaginary part non zero. As a consequence, even when accouting for stabilizing terms such as drag terms, the numerical approximations may blow up when the mesh is refined, even if stabilizing upwinding techniques are used in the overall algorithm. This is clearly demonstrated in[17,21] for instance. The inclusion of some additional terms may only slightly increase the space of hyperbolic states (see[24]). Based on these facts, one may wonder whether the numerical prediction is feasable for these models, at least on coarse meshes. Actually, most of existing algorithms that are used to compute approximations of such models are derived from the single-phase Navier-Stokes like schemes, which basically rely on a predictor-corrector step, where the stabilizing step computes approximations of the mean pressure field in such a way that acoustic waves are correctly predicted. They are commonly refered to as pressure-correction algorithms. Of course, when the flow locally enters some non-hyperbolic region, a refinement of the mesh also leads to a blow-up of the numerical approximation.

The main underlying ideas of our approach are quite different. First of all, we do not wish to restrict our framework of physical models to the current single-pressure formalism. A second point is linked with the fact that we wish to have a straightforward way to construct schemes, in a simple manner that will render the computations cheap enough. An obvious way to achieve this is discussed below. It simply consists in getting rid of the local instantaneous pressure equilibrium assumption. Once that is admitted, the solution naturally arises : it only remains to find some father model of PDEs which comply with the two requirements:

- the initial value problem associated with the father model should be well-posed ;
- the father model should allow retrieving the classical three-phase flow model when assuming the instantaneous pressure equilibrium.

A similar approach has been considered before in order to tackle two-phase flows. Actually, one admissible father model corresponds to the Baer-Nunziatto model (see[1]), or equivalently to models investigated in[2,13,22] . Some properties of these models are detailed in[10] , and an important item to be quoted is that these models guarantee a unique set of jump conditions (see[7]).

III. The hyperbolic three-phase flow model

The father model detailed below ensures that a physically relevant entropy inequality holds, but it also guarantees that a unique set of meaningful jump conditions holds, as occurs in the two-phase framework. As explained in[20] (appendix G), the combination of the latter two constraints on: (i) the entropy balance and: (ii) the existence of a unique set of relevant jump conditions, reduces the admissible choices to a few expressions for V_i.

The governing equations of the hyperbolic three-phase flow model read (see[19,20] for further details) :

$$\alpha_1 + \alpha_2 + \alpha_3 = 1 \tag{6}$$

$$\frac{\partial \alpha_k}{\partial t} + V_i \frac{\partial \alpha_k}{\partial x} = \phi_k \tag{7}$$

$$\frac{\partial \alpha_k \rho_k}{\partial t} + \frac{\partial \alpha_k \rho_k U_k}{\partial x} = 0 \tag{8}$$

$$\frac{\partial \alpha_k \rho_k U_k}{\partial t} + \frac{\partial \alpha_k (\rho_k U_k^2 + P_k)}{\partial x} + \sum_{l=1, l\neq k}^{3} P_{kl} \frac{\partial \alpha_l}{\partial x} = S_{U_k} \tag{9}$$

$$\frac{\partial \alpha_k E_k}{\partial t} + \frac{\partial \alpha_k U_k (E_k + P_k)}{\partial x} - \sum_{l=1, l\neq k}^{3} P_{kl} \frac{\partial \alpha_l}{\partial t} = V_i S_{U_k} \tag{10}$$

still noting $\alpha_k E_k = m_k e_k(P_k, \rho_k) + m_k U_k^2/2$ (for $k = 1, 2, 3$) with the additional constraints:

$$\phi_1 + \phi_2 + \phi_3 = 0 \tag{11}$$

$$P_{12} + P_{32} = P_{13} + P_{23} = P_{21} + P_{31} \tag{12}$$

The condition (11) guarantees the compatibility with the constraint (6). Meanwhile, the condition (12) arises from the fact that non-conservative contributions of the left hand side of (9) and (10) represent interfacial transfer terms, which means that the sum over all phases must cancel.

In order to obtain a closed set of equations, one needs to precise the exact form of the interface velocity V_i, the six unknowns P_{kl}, and the three closures for ϕ_k. We consider here the following set :

$$V_i = U_1 \tag{13}$$

$$\phi_k = f_{1-k} \alpha_1 \alpha_k (P_k - P_1)/(P_1 + P_2 + P_3) \quad \text{for} \quad k = 2, 3 \tag{14}$$

$$P_{12} = P_{23} = P_{21} = P_2 \tag{15}$$

$$P_{13} = P_{31} = P_{32} = P_3 \tag{16}$$

The frequencies f_{1-k} must remain bounded over $\Omega \times [0, T]$. We also need to close drag terms in a standard way (for $k = 2, 3$):

$$S_{U_k} = \psi_k (U_1 - U_k) \tag{17}$$

where the drag coefficients ψ_k should of course remain positive.

The system ((6)-(10)) complies with the above mentionned requirements:

- the convective subset associated with the father model ((6)-(10)) is hyperbolic for any physically meaningful state ;

- some algebra enables to check very quickly that it enables to retrieve the classical three-phase flow model ((2) - (4)) while inserting $P_1 = P_2 = P_3$ (noted P) in ((7) - (10)).

We may thus turn now to the numerical procedure, which uses the Finite Volume approach.

IV. The relaxation method

The overall approach consists in two seperate steps :

- (i) An evolution step,
- (ii) A relaxation step that accounts for drag effects and enables a return to a pressure equilibrium between phases.

A. The evolution step:

The evolution step corresponds to the convective step ((18)-(21)):

$$\frac{\partial \alpha_k}{\partial t} + V_i \frac{\partial \alpha_k}{\partial x} = 0 \tag{18}$$

$$\frac{\partial \alpha_k \rho_k}{\partial t} + \frac{\partial \alpha_k \rho_k U_k}{\partial x} = 0 \tag{19}$$

$$\frac{\partial \alpha_k \rho_k U_k}{\partial t} + \frac{\partial \alpha_k (\rho_k U_k^2 + P_k)}{\partial x} + \sum_{l=1, l\neq k}^{3} P_{kl} \frac{\partial \alpha_l}{\partial x} = 0 \tag{20}$$

$$\frac{\partial \alpha_k E_k}{\partial t} + \frac{\partial \alpha_k U_k (E_k + P_k)}{\partial x} - \sum_{l=1, l\neq k}^{3} P_{kl} \frac{\partial \alpha_l}{\partial t} = 0 \tag{21}$$

(for $k = 1, 2, 3$).

Property 1

- The convective subset is hyperbolic. The structure of fields in the Riemann problem associated with the convective step guarantees that void fractions α_k, mass fractions m_k and internal energies remain positive for $k = 1, 2, 3$ (see[20]).
- The jump conditions are uniquely defined.

We only detail here the form of eigenvalues, which are:

$$\left\{ \begin{array}{lll} \lambda_1 = U_1 - c_1, & \lambda_{2,3,4} = U_1 & \lambda_5 = U_1 + c_1 \\ \lambda_6 = U_2 - c_2, & \lambda_7 = U_2, & \lambda_8 = U_2 + c_2 \\ \lambda_9 = U_3 - c_3, & \lambda_{10} = U_3, & \lambda_{11} = U_3 + c_3 \end{array} \right. \tag{22}$$

We may thus compute approximations of solutions of the evolution step, and this is achieved by a straightforward integration of the subset on cells, using either the Rusanov scheme, or the approximate Godunov scheme VFRoe-ncv[3] . The time step is chosen in agreement with the CFL condition for explicit approximations. For a regular mesh, this one is: $\Delta t^n max_i(|U|_k + c_k)_i < h$, for $k = 1, 2, 3$. Other upwinding techniques (see[14,15] or[4,25]) may of course be used within this step.

A very important point to be quoted is that *approximate solutions* of the latter convective systems *converge towards the same solution when the mesh is refined, whatever the numerical scheme is*[17] (Rusanov scheme, aproximate Godunov scheme, ...). This is due to the fact that jump conditions are well defined (see property 1.*b*), though non conservative contributions are present in the set of PDE. This is a remarkable property that standard three-fluid (and also standard two-fluid) models do not enjoy. It is mainly due to the fact that the interface velocity ensures that the field associated with the eigenvalue V_i is linearly degenerated (see[19,20] and[7,10] for the counterpart in two-phase flows), and to the structure of the solution of the one-dimensional Riemann problem.

B. The relaxation step:

The computation of approximations of the relaxation step is achieved by means of two substeps.

1. *Physical relaxation:*

Drag effects are accounted for within the first substep:

$$\frac{\partial \alpha_k}{\partial t} = \frac{\partial \alpha_k \rho_k}{\partial t} = 0 \tag{23}$$

$$\frac{\partial \alpha_k \rho_k U_k}{\partial t} = S_{U_k} \tag{24}$$

$$\frac{\partial \alpha_k E_k}{\partial t} = V_i S_{U_k} \tag{25}$$

with $\alpha_1 + \alpha_2 + \alpha_3 = 1$. We emphasize that the mass transfer terms may be accounted for within this step if necessary. This step makes pressures increase within each phase. Actually, owing to the last three equations, the variation of the pressure P_k within the step reads:

$$m_k \frac{\partial e_k(P_k, \rho_k)}{\partial t} = (V_i - U_k) S_{U_k} = \psi_k (U_1 - U_k)^2 > 0 \tag{26}$$

for $k = 2, 3$, whereas $\dfrac{\partial P_1}{\partial t} = 0$. Hence, the thermodynamical condition $\dfrac{\partial e_k}{\partial P_k}|_{\rho_k} > 0$ guarantees positive values of P_k, for $k = 1, 2, 3$, assuming that initial conditions are physically relevant. The discrete counterpart may of course be easily obtained using Finite Volume methods. We do not detail here the computation of the first substep in the relaxation step and we refer for instance to[10] .

2. *Pressure relaxation*

This requires to specify whether one computes the standard three-phase flow model or the hyperbolic model. The reader is also refered to[23] for various relaxation procedures.

- *Standard three-field model*
  In that case, an instantaneous pressure equilibirum is achieved while computing:

$$\frac{\partial \alpha_k}{\partial t} = \phi_k \tag{27}$$

$$\frac{\partial \alpha_k \rho_k}{\partial t} = \frac{\partial \alpha_k \rho_k U_k}{\partial t} = 0 \tag{28}$$

$$\frac{\partial \alpha_k E_k}{\partial t} - \sum_{l=1, l \neq k}^{3} P_{kl} \frac{\partial \alpha_l}{\partial t} = 0 \tag{29}$$

  assuming $(f_{1-k})^{-1} = 0$. Actually, for each cell indexed by subscript i, and for given $\tilde{f}$ values at the beginning of the pressure relaxation step, we compute (we set here : $f_{2-3}(W) = 0$ to simplify the presentation):

$$(P_k)_i^{n+1} = P_i^{n+1} \tag{30}$$

$$(m_k)_i^{n+1} = (\tilde{m_k})_i \tag{31}$$

$$(m_k U_k)_i^{n+1} = (\tilde{m_k U_k})_i \tag{32}$$

$$(\alpha_k E_k)_i^{n+1} - (\tilde{\alpha_k E_k})_i + P_i^{n+1}((\alpha_k)_i^{n+1} - (\tilde{\alpha_k})_i) = 0 \tag{33}$$

  Hence, by accounting for the first three mesh schemes, the fourth equation provides:

$$(m_k e_k)_i^{n+1} - (\tilde{m_k e_k})_i + P_i^{n+1}((\alpha_k)_i^{n+1} - (\tilde{\alpha_k})_i) = 0$$

If we moreover restrict to perfect gas EOS within each step, setting: $(\gamma_k - 1)\rho_k e_k = P_k$ (with: $\gamma_k - 1 > 0$), we get the final form of the equilibrium pressure:

$$(P_k)_i^{n+1} = P_i^{n+1} = \frac{\gamma_2\gamma_3(\alpha_1\tilde{P_1})_i + \gamma_1\gamma_3(\alpha_2\tilde{P_2})_i + \gamma_1\gamma_2(\alpha_3\tilde{P_3})_i}{\gamma_2\gamma_3(\tilde{\alpha_1})_i + \gamma_1\gamma_3(\tilde{\alpha_2})_i + \gamma_1\gamma_2(\tilde{\alpha_3})_i}$$

Meanwhile the updated cell values of void fractions are:

$$(\alpha_k)_i^{n+1} = (\tilde{\alpha}_k)_i(\frac{\gamma_k - 1}{\gamma_k} + \frac{(\tilde{P_k})_i}{\gamma_k P_i^{n+1}})$$

This step is the straightforward counterpart of the one introduced in[6] . It is exactly the same that has been used in[21] in order to compute two-phase flow models. It enjoys interesting properties as summarized below.

- *Hyperbolic three-phase flow model*
  One of the main differences between the hyperbolic three-phase flow model and the standard three-phase flow model is due to the fact that time scales $(f_{1-k})^{-1}$ involved in the hyperbolic model are non zero. For the hyperbolic model, we note that a return to a pressure equilibrium is ensured in the long time limit. Actually, if one notes :

$$a_k = \frac{\partial e_k(P_k, \rho_k)}{\partial P_k} \quad \text{and} \quad d_k = f_{1-k}P_k\alpha_1\alpha_k/(P_1 + P_2 + P_3) \tag{34}$$

$$X = P_1 - P_2 \quad \text{and} \quad Y = P_1 - P_3 \tag{35}$$

  one can show that :

$$\frac{1}{2}(d_2\frac{\partial X^2}{\partial t} + d_3\frac{\partial Y^2}{\partial t}) = -\frac{(d_2X)^2}{m_2a_2} - \frac{(d_3Y)^2}{m_3a_3} - \frac{(d_2X + d_3Y)^2}{m_1a_1} \leq 0 \tag{36}$$

  which means that non-zero time scales involved in ϕ_k contribute to a return towards equilibrium for the three pressure fields. We do not detail here the computation of pressures and void fractions, since this step is exactly the counterpart of the one detailed in.[10]

C. Main properties of the scheme:

The main properties of the evolution step are:

Property 2:

- The Rusanov scheme enables to maintain positive values of the void fraction and partial masses, assuming a standard CFL condition.
- The exact Godunov scheme guarantees positive values of void fractions, densities and internal energies.

The main properties of the relaxation process are the following:

Property 3:

- The first substep in the relaxation process ensures positive values of void fractions, mass fractions and pressures P_k.
- When focusing either on the standard three-field model, assuming instantaneous pressure relaxation, or on the hyperbolic three-phase flow model, the second substep in the relaxation process is such that:
  - It preserves positive values of void fractions and mass fractions,
  - Positive cell values of the equilibrium presssure are guaranteed,
  - It is consistent with respect to pressure, since:
    $(\tilde{P_1})_k = (\tilde{P_2})_k = (\tilde{P_3})_k = p$ implies : $(P_1)_k^{n+1} = (P_2)_k^{n+1} = (P_3)_k^{n+1} = p$.

V. Numerical results

We restrict to two simple test cases.

The first one corresponds to the behaviour of the flow close to wall boundaries. The flow is computed with the standard single-pressure model on a mesh including 20000 cells. A modified Lax-Friedrichs scheme has been used to compute the evolution step, and the instantaneous pressure relaxation step (30) has been applied. We use perfect gas EOS within each phase :$(\gamma_k - 1)\rho_k e_k = P_k$. On each side of the middle of the computational domain -corresponding to the wall location-, the initial conditions:
$(\alpha_2)_L = 0.4$, $(\alpha_3)_L = 0.5$, $(\alpha_2)_R = 0.4$, $(\alpha_3)_R = 0.5$,
$(U_1)_L = 1$, $(\rho_1)_L = 70$, $(P_1)_L = 1.5 \quad 10^7$, $(U_1)_R = -1$, $(\rho_1)_R = 70$, $(P_1)_R = 1.5 \quad 10^7$,
$(U_2)_L = 1$, $(\rho_2)_L = 700$, $(P_2)_L = 1.5 \quad 10^7$, $(U_2)_R = -1$, $(\rho_2)_R = 700$, $(P_2)_R = 1.5 \quad 10^7$,
$(U_3)_L = 1$, $(\rho_3)_L = 700$, $(P_3)_L = 1.5 \quad 10^7$, $(U_3)_R = -1$, $(\rho_3)_R = 700$, $(P_3)_R = 1.5 \quad 10^7$.
generate a flow that will hit the wall boundary. This results in a solution that includes shock wave patterns as displayed in figures (1), (2) and (3). We note that the void fraction of the light phase labelled 1 close to the wall is weaker, whereas it increases for the heavier phases $2, 3$, which was expected.

The second one shows a comparison of both models when simulating a shock tube experiment on a rather coarse mesh with 200 cells. The initial conditions are now :
$(\alpha_2)_L = 0.4$, $(\alpha_3)_L = 0.5$, $(\alpha_2)_R = 0.5$, $(\alpha_3)_R = 0.4$,
$(U_1)_L = 0$, $(\rho_1)_L = 1$, $(P_1)_L = 10^5$, $(U_1)_R = 0$, $(\rho_1)_R = 0.125$, $(P_1)_R = 10^4$,
$(U_2)_L = 0$, $(\rho_2)_L = 1$, $(P_2)_L = 10^5$, $(U_2)_R = 0$, $(\rho_2)_R = 0.125$, $(P_2)_R = 10^4$,
$(U_3)_L = 0$, $(\rho_3)_L = 1$, $(P_3)_L = 10^5$, $(U_3)_R = 0$, $(\rho_3)_R = 0.125$, $(P_3)_R = 10^4$.
on each side of the membrane located at the middle of the computational domain. The main objective here is to examine the impact of pressure relaxation assuming very weak drag contributions and rather low frequencies f_{1-k} - or conversely long time scales for a return to a pressure equilibrium-. We note that the discrepancies between solutions are far less than what one might expect (see figure (4)). These become even lower when drag coefficients are representative of two clouds of small particles in a gas medium, or of small bubbles in a continuous liquid phase. Moreover, the available data for f_{1-k} suggests that true values are much higher than values used in this test case, and almost make these discrepancies vanish. This is in agreement with results presented in[17] . It also suggests that a smooth transition between both models is feasable for industrial purposes.

VI. Conclusion

We thus have a two-fold conclusion:

(i) The numerical method which has been proposed herein, which combines the use of the three-phase approach and the relaxation procedure, enables to cope with both the three-phase flow model and the standard three-field model, without specific restriction on the time stepping ;

(ii) The algorithm is stable when the initial-value problem is well-posed, and it does not hide deficiencies of continuous models that enter a time-elliptic region (see[21]).

It may thus be seen as a possible tool to compute both well-posed initial-value problems on any mesh size, and possibly locally ill-posed models on "coarse meshes", using almost the same numerical procedure.

The extension of these results for applications in a porous medium is straightforward (see[12]).

Acknowledgments

This work has been achieved in the framework of the NEPTUNE project (see[16]), financially supported by CEA (Commissariat à l'Energie Atomique), EDF (Electricité de France), IRSN (Institut de Radioprotection et Sureté Nucléaire) and AREVA-NP. Computational facilities were provided by EDF.

References

[1]M.R. Baer and J.W. Nunziato, A two phase mixture theory for the deflagration to detonation transition (DDT) in reactive granular materials, *Int. J. Multiphase Flow*, vol. 12-6, pp. 861–889, 1986.

[2]J.B. Bdzil, R. Menikoff, S.F. Son, A.K. Kapila and D.S. Stewart, Two phase modeling of a deflagration-to-detonation transition in granular materials: a critical examination of modeling issues, *Phys. of Fluids* , vol. 11, pp. 378–402, 1999.

[3]T. Buffard, T. Gallouët and J.M. Hérard, A sequel to a rough Godunov scheme. Application to real gas flows, *Computers and Fluids*, vol. 29-7, pp. 813–847, 2000.

[4]C.E. Castro and E.F. Toro, A Riemann solver and upwind methods for a two-phase flow model in non-conservative form, *Computers and Fluids*, vol. 35, pp. 275–307, 2006.

[5]Z. Chen and R.E. Erwing, Comparison of various formulations of three-phase flows in porous media, *J. of Comp. Phys.*, vol. 132, pp 362–373, 1997.

[6]F. Coquel, K. El Amine, E. Godlewski, B. Perthame and P. Rascle, A numerical method using upwind schemes for the resolution of two phase flows, *J. of Comp. Phys.*, vol. 136, pp 272–288, 1997.

[7]F. Coquel, T. Gallouët, J.M. Hérard and N. Seguin, Closure laws for a two fluid two-pressure model, *C. R. Acad. Sci. Paris*, vol. I-332, pp. 927–932, 2002.

[8]D.A. Drew and S.L. Passman, *Theory of multi-component fluids*, Applied Mathematical Sciences, vol. 135, 1999.

[9]H. Frid and V. Shelukhin, A quasi linear parabolic system for three phase capillary flow in porous media, *SIAM J. of Math. Anal.*, vol. 33, pp 1029–1041, 2003.

[10]T. Gallouët, J.M. Hérard and N. Seguin, Numerical modelling of two phase flows using the two-fluid two-pressure approach, *Math. Mod. Meth. Appl. Sci.*, vol. 14, n°5, pp. 663-700, 2004.

[11]S. Gavrilyuk, Acoustic properties of a two-fluid compressible mixture with micro-inertia, *European J. of Mechanics / B*, vol. 24-3, pp. 397-406, 2005.

[12]S. Gavrilyuk and J.M. Hérard, *in preparation.*

[13]S. Gavrilyuk and R. Saurel, Mathematical and numerical modelling of two-phase compressible flows with micro inertia, *J. of Comp. Phys.* , vol.175, pp.326 -360, 2002.

[14]E. Godlewski and P.A. Raviart, *Numerical approximation for hyperbolic systems of conservation laws*, Springer Verlag, 1996.

[15]S.K. Godunov, A difference method for numerical calculation of discontinous equations of hydrodynamics, *Sbornik*, pp. 271–300. In Russian, 1959.

[16]A. Guelfi, D. Bestion, M. Boucker, P. Fillion, M. Grandotto, J.M. Hérard, E. Hervieu and P. Peturaud, NEPTUNE: a new software platform for advanced nuclear thermal hydraulics, *Nuclear Science and Engineering*, vol. 156, 2007

[17]V. Guillemaud, Modélisation et simulation numérique des écoulements diphasiques par une approche bifluide à deux pressions, in French, *PhD thesis*, Université Aix-Marseille I, Marseille, France, March 27, 2007.

[18]J.M. Hérard, Numerical modelling of turbulent two phase flows using the two-fluid approach, *AIAA paper 2003-4113*, 2003.

[19]J.M. Hérard, A hyperbolic three-phase flow model, *Comptes Rendus Académie des Sciences de Paris, Série Mathématique*, I-342, pp. 779–784, 2006.

[20]J.M. Hérard, A three-phase flow model, *Mathematical and Computer Modelling*, vol. 45, pp. 732-755, 2007.

[21]J.M. Hérard and O. Hurisse, A relaxation method to compute two-fluid models, *Int. J. of Comp. Fluid Dyn.*, vol. 19, pp. 475-482, 2005.

[22]A.K. Kapila, R. Menikoff, J.B. Bdzil, S.F. Son and D.S. Stewart, Two-phase modeling of DDT in granular materials: reduced equations, *Phys. of Fluids*, vol. 13, pp. 3002–3024, 2001.

[23]M.H. Lallemand, A. Chinnayya and O. Le Metayer, Pressure relaxation procedures for multiphase compressible flows, *Int. J. for Numerical Methods in Fluids*, vol. 49, pp. 1–56, 2005.

[24]S.T. Munkejord, Comparison of Roe-type methods for solving the two-fluid model with and without pressure relaxation, *Computers and Fluids*, vol. 36, pp. 1061–1080, 2007.

[25]D.W. Schewendeman, C.W. Wahle and A.K. Kapila, The Riemann problem and high-resolution method Godunov method for a model of compressible two-phase flow, *J. of Comp. Phys.* , vol.212, pp.490 -256, 2006.

[26]S. Jayanti and M. Valette, Prediction of dryout and post dry-out heat transfer at high pressure using a one-dimensional three-field model, *Int. J. of Heat and Mass Transfer*, vol.47-22, pp. 4895-4910, 2004.

The wall is located at x=10000

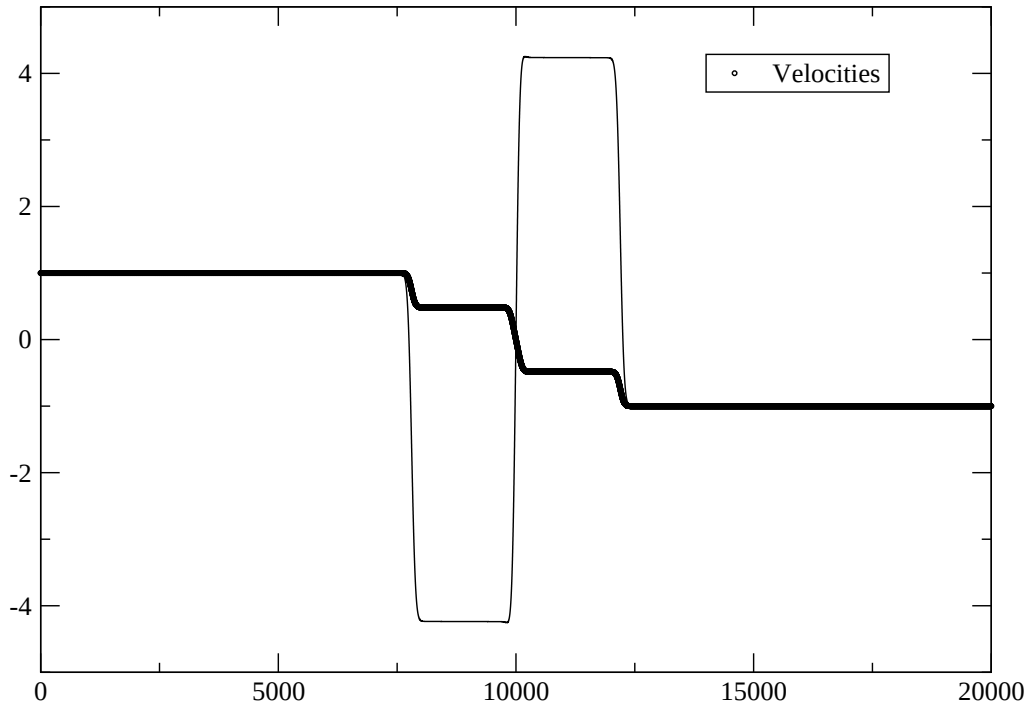

Figure 1. Standard three-fluid model - Velocity fields when the flow hits a wall boundary. U1 (plain line), U2 (dotted line), U3 (circles)

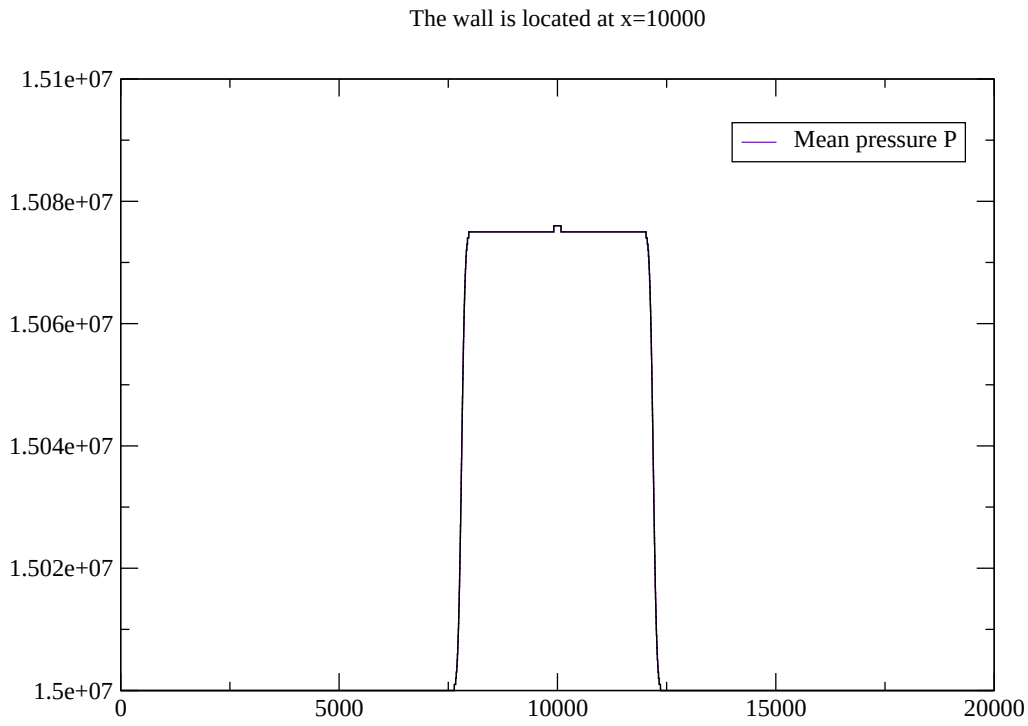

Figure 2. Standard three-fluid model - Mean pressure field P when the flow hits a wall boundary.

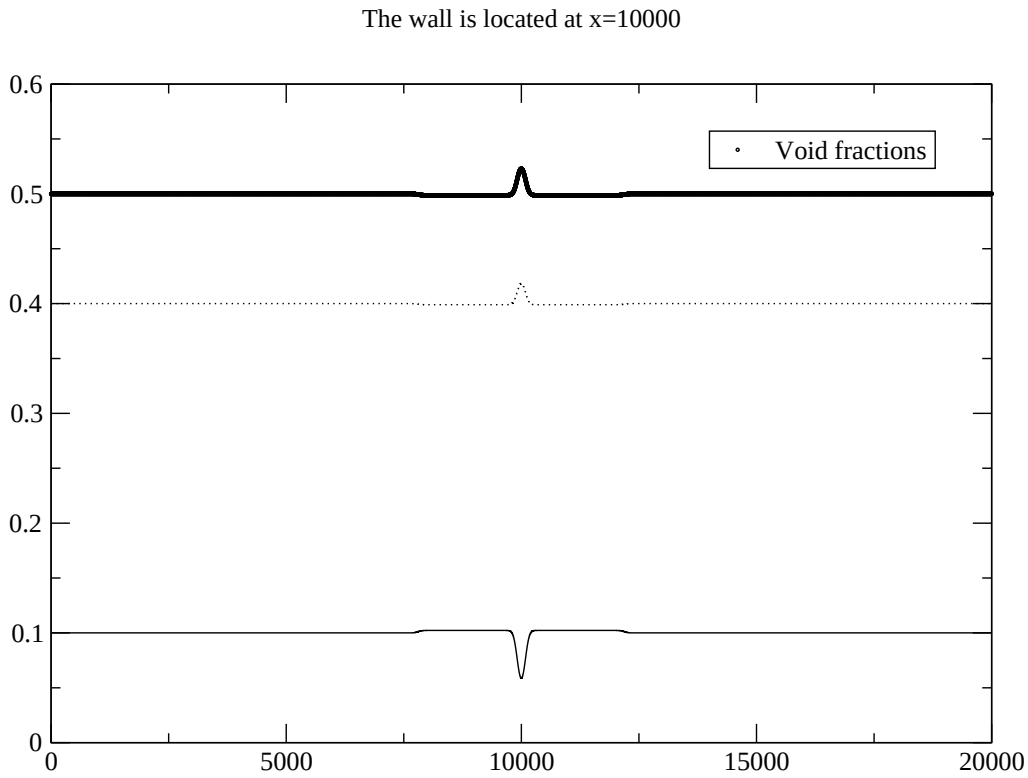

Figure 3. Standard three-fluid model - Void fraction distribution when the flow hits a wall boundary. α_1 (plain line), α_2 (dotted line), α_3 (circles)

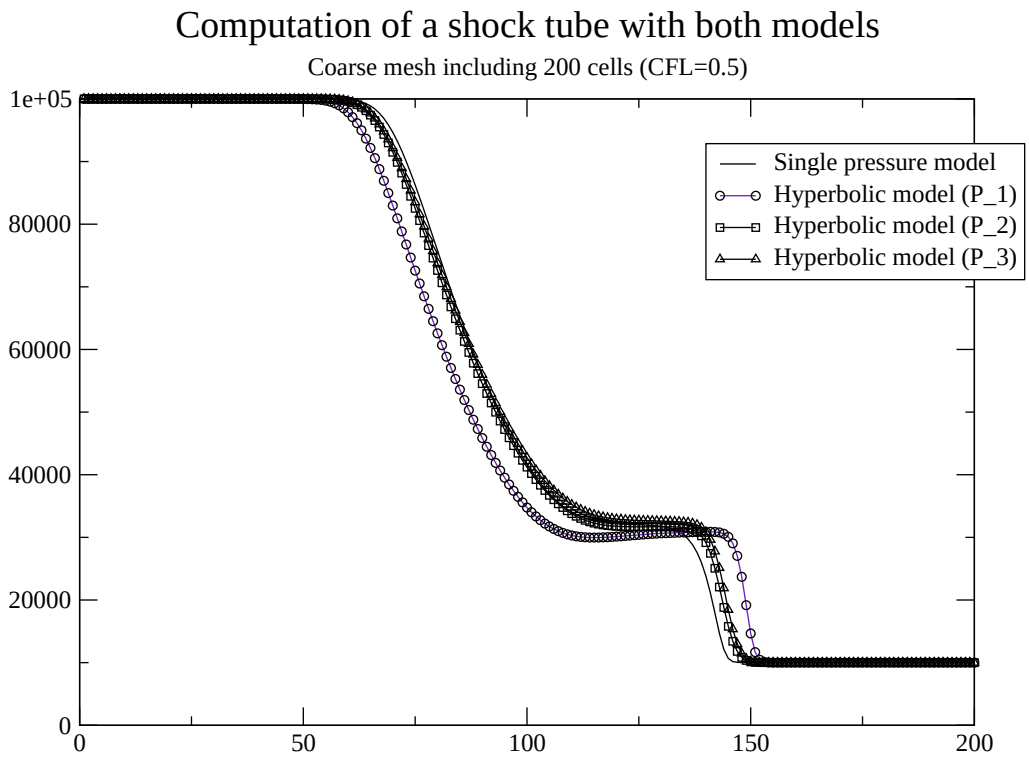

Figure 4. Shock tube experiment. Both approaches are compared using very large relaxation time scales for pressure and velocity fields.